International Journal of Thermophysics, Vol. 18, No. 3, 1997

Equation of State for Gaseous Propane Determined from the Speed of Sound

J. P. M. Trusler[1]

Received July 21, 1996

An equation of state in the form of a truncated virial series has been developed for gaseous propane. Second, third, and fourth virial coefficients and their temperature derivatives were calculated from model two- and three-body intermolecular potentials, the parameters of which were fitted to experimental values of the speed of sound in the gas; no other data were used. The resulting model predicts accurately thermal and caloric properties of the gas over a wide range of temperatures at densities up to about one-quarter of the critical. The second and third (but not the fourth) virial coefficients are in very close agreement with directly measured values. To facilitate rapid calculation of thermodynamic properties, a look-up table for the virial coefficients and their temperature derivatives is provided together with a recommended means of interpolation.

KEY WORDS: equation of state; propane; speed of sound; virial coefficients.

1. INTRODUCTION

With sufficient attention to experimental method, it is possible to make measurements of the speed of sound in a gas with probably greater precision and accuracy than can be achieved for any other thermodynamic property [1–3]. Consequently, the results of such experiments can form both a very sensitive test of existing equations of state and an extremely valuable input to the development of new equations of state. Conventionally, sound-speed data, where available, are considered along with a wide range of other thermodynamic properties in the development of empirical equations of state. This approach reflects both the desire to represent all experimental data to within their uncertainties and the fact that it

[1] Department of Chemical Engineering and Chemical Technology, Imperial College, Prince Consort Road, London SW7 2BY, United Kingdom.

0195-928X/97/0500-0635$12.50/0

is formally impossible to base an equation of state, even for a single homogeneous phase, on speeds of sound alone; this remains true whatever the accuracy of the data.

To determine most other thermodynamic properties from the speed of sound, independent initial conditions are required as input to an integration of the differential equations which link the speed of sound to the pVT surface [2, 3]. When initial conditions are available, that approach may be used to advantage as has been demonstrated by recent results for methane [2], ethane [4], and argon [5].

It is possible numerically to propose an empirical parameterisation of the pVT surface and to fit it to sound-speed data alone. However, as no initial conditions are specified in this method, there is no guarantee that the resulting pVT surface is correct even if the speed of sound is accurately reproduced. Indeed, there is evidence that, with purely empirical parameterisations, the pVT surface may contain quite large errors while still providing a substancially correct representation of the speed of sound [6]. Thus while this procedure may be useful in some cases, it is unsuitable for obtaining results of very high accuracy. Nevertheless, it seems likely that the situation can be improved dramatically by the adoption of a theoretically based equation of state which has the "correct" functional form. For example, a perturbed hard-sphere equation of state fitted to the speed of sound in helium was shown to provide a good representation of the pVT surface over a very wide range of conditions [7]. Some recent results for methane, based on square-well intermolecular potentials, are also encouraging [10].

At low densities, the pVT surface is known to reduce to the virial equation of state, the coefficients of which may be determined from the intermolecular potential-energy functions pertaining to clusters of two, three, four,... molecules at a time. The present work, which builds on previous studies [8–10], was undertaken with the objective of establishing a virial equation of state for gaseous propane that would be useful over a wide range of temperatures and at densities up to some appreciable fraction of the critical. The second, third, and fourth virial coefficients are determined from prescribed two- and three-molecule model potentials, the parameters of which were fitted to the sound speed data reported recently by Trusler and Zarari [11]. Higher virial coefficients are neglected.

2. THEORY

The speed of sound u is given by the well-known equation

$$u^2 = M^{-1}(\partial p/\partial \rho_n)_S \tag{1}$$

where p is the pressure, ρ_n is the amount-of-substance density, M is the molar mass, and S is the entropy. In terms of the compression factor $Z = p/\rho_n RT$ and its isothermal and isochoric partial derivatives, Eq. (1) becomes

$$u^2 = (RT/M)[\{Z + \rho_n(\partial Z/\partial \rho_n)_T\} + (R/C_{V,m})\{Z + T(\partial Z/\partial T)_{\rho_n}\}^2] \quad (2)$$

Here $C_{V,m}$ is the molar isochoric heat capacity, which, for a gas, may written

$$C_{V,m} = C^{pg}_{V,m} - R\int_0^{\rho_n} \{2T(\partial Z/\partial T)_{\rho_n} + T^2(\partial^2 Z/\partial T^2)_{\rho_n}\}\, \rho_n^{-1}\, d\rho_n \quad (3)$$

where $C^{pg}_{V,m}$ is the molar isochoric heat capacity of the perfect gas. The equation of state of a gas may be written

$$Z = 1 + B_2\rho_n + B_3\rho_n^2 + B_4\rho_n^3 + \cdots \quad (4)$$

where B_N $(N = 2, 3, 4, \ldots)$ are virial coefficients that depend upon temperature only for a gas of constant composition. In terms of this equation of state, we have

$$Z + \rho_n(\partial Z/\partial \rho_n)_T = 1 + 2B_2\rho_n + 3B_3\rho_n^2 + 4B_4\rho_n^3 + \cdots \quad (5a)$$

$$Z + T(\partial Z/\partial T)_{\rho_n} = 1 + (B_2 + TB_2^{(1)})\,\rho_n + (B_3 + TB_3^{(1)})\,\rho_n^2 + (B_4 + TB_4^{(1)})\,\rho_n^3 + \cdots \quad (5b)$$

$$(C_{V,m} - C^{pg}_{V,m})/R = -(2TB_2^{(1)} + T^2B_2^{(2)})\,\rho_n - \tfrac{1}{2}(2TB_3^{(1)} + T^2B_3^{(2)})\,\rho_n^2 - \tfrac{1}{3}(2TB_4^{(1)} + T^2B_4^{(2)})\,\rho_n^3 - \cdots \quad (5c)$$

where $B_N^{(i)}$ denotes the ith temperature derivative of B_N.

It is well-known from statistical mechanics that the virial coefficients are related to the potential energy surfaces of clusters containing two, three, four,... molecules at a time [12]. An important simplification arises for rigid (as opposed to flexible) molecules, as in this case the potential energy may be separated unambiguously into intra- and intermolecular parts; the virial coefficients are then determined by the latter alone. Further simplification arises if one assumes that the intermolecular potential energy is determined only by the positions of the centres of mass, although this is strictly true only for spherical molecules. We may then write the total intermolecular potential energy U of a cluster of N molecules as

$$U = \sum_{i=1}^{N-1} \sum_{j=i+1}^{N} \phi(r_{ij}) + \Delta\phi_N \quad (6)$$

where r_{ij} is the distance between molecule i and molecule j. In Eq. (6), ϕ is the intermolecular potential-energy function of an isolated pair of molecules and $\Delta\phi_N$ is the difference between the total potential energy and the sum of the pair interaction energies in a cluster of N molecules with $N \geqslant 3$.

The present work is concerned with propane which is neither rigid nor spherical. However, as a working hypothesis, it has been assumed that an accurate representation of the virial coefficients may be obtained by adopting the spherically symmetric intermolecular potential model:

$$\phi(r)/\varepsilon = \{6/(n-6)\}(r_m/r)^n - \{n/(n-6)\}(r_m/r)^6 \tag{7}$$

This potential, proposed by Maitland and Smith [13], contains the following four parameters: ε, the depth of the potential well; r_m, the separation at which $\phi = -\varepsilon$; and the shape parameters m and γ, which determine the exponent n through the linear equation

$$n = m + \gamma\{(r/r_m) - 1\} \tag{8}$$

It is also assumed that (a) only three-body contributions to $\Delta\phi_N$ need be considered; (b) for purposes of evaluating four-molecule cluster-integrals the exponential of $-\Delta\phi_4/kT$ may be approximated by [14]

$$\exp(-\Delta\phi_4/kT) \approx 1 + f_{123} + f_{124} + f_{134} + f_{234} \tag{9}$$

and (c) $\Delta\phi_3$ is given by the Axilrod–Teller triple-dipole term:

$$\Delta\phi_3 = \nu_{123}(r_{12}^3 r_{13}^3 r_{23}^3)^{-1}(1 + 3\cos\theta_1 \cos\theta_2 \cos\theta_3) \tag{10}$$

Here, $f_{ijk} = \exp\{-\Delta\phi_3(r_{ij}, r_{ik}, r_{jk})/kT\} - 1$, θ_i is defined as the angle subtended at molecule i by molecules j and k, and ν_{123} is a dispersion coefficient.

The virial coefficients B_2, B_3, and B_4 are given by [12, 14]

$$B_2 = -(L/2V)\int_V f_{12}\, d\mathbf{r}_1\, d\mathbf{r}_2 \tag{11}$$

$$B_3 = -(L^2/3V)\int_V (f_{12}f_{13}f_{23} - e_{12}e_{13}e_{23}f_{123})\, d\mathbf{r}_1\, d\mathbf{r}_2\, d\mathbf{r}_3 \tag{12}$$

$$B_4 = -(L^3/8V)\int_V \{f_{12}f_{23}f_{34}f_{14}(3 + 6f_{13} + f_{13}f_{24}) - 4e_{12}e_{13}e_{23}(3f_{24}f_{34} + f_{14}f_{24}f_{34})f_{123}\}\, d\mathbf{r}_1\, d\mathbf{r}_2\, d\mathbf{r}_3\, d\mathbf{r}_4 \tag{13}$$

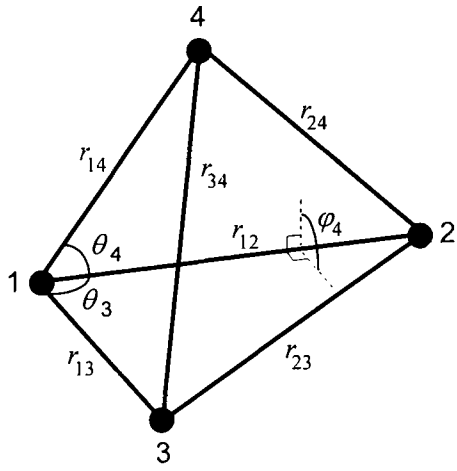

Fig. 1. Coordinate system for a cluster of four molecules (φ_4 is the angle between plane 123 and plane 124).

where L is Avagadro's constant, V is volume, $\mathbf{r}_i$ is the position vector of molecule i, $e_{ij}=\exp\{-\phi(r_{ij})/kT\}$, and $f_{ij}=e_{ij}-1$. Expressions for the required temperature derivatives $B_N^{(i)}$ are not given here, as they are rather lengthy, but are easily obtained by differentiation of the integrands in Eqs. (11)–(13).

For computational purposes, the variables of integration may be expressed in terms of the lengths and angles defined in Fig. 1 as

$$\left.\begin{aligned} V^{-1}\int_V d\mathbf{r}_1\, d\mathbf{r}_2 &= 4\pi\int_0^\infty r_{12}^2\, dr_{12} \\ V^{-1}\int_V d\mathbf{r}_1\, d\mathbf{r}_2\, d\mathbf{r}_3 &= 8\pi^2\int_0^\infty r_{12}\, dr_{12}\int_0^\infty r_{13}\, dr_{13}\int_{|r_{12}-r_{13}|}^{r_{12}+r_{13}} r_{23}\, dr \\ V^{-1}\int_V d\mathbf{r}_1\, d\mathbf{r}_2\, d\mathbf{r}_3\, d\mathbf{r}_4 &= 8\pi^2\int_0^\infty r_{12}^2\, dr_{12}\int_0^\infty r_{13}^2\, dr_{13}\int_0^\infty r_{23}^2\, dr_{23} \\ &\quad\times\int_{-1}^1 d(\cos\theta_3)\int_{-1}^1 d(\cos\theta_4)\int_0^{2\pi} d\varphi_4 \end{aligned}\right\} \quad (14)$$

3. NUMERICAL METHODS

Parameters in the model pair and triplet potentials were determined in a nonlinear regression analysis which minimized the dimensionless χ^2 statistic defined by

$$\chi^2 = \frac{\sum_{i=1}^{N} \{u_i - u_{\text{fit}}(T_i, p_i)\}^2 / s_i^2}{N - N_{\text{P}}} \tag{15}$$

Here u_i is the ith experimental speed of sound, s_i is the estimated standard deviation of u_i, u_{fit} is the speed of sound calculated from the model at the ith state point, N is the total number of points, and N_{P} is the number of parameters.

$u_{\text{fit}}(T_i, p_i)$ was calculated in the following way. First, the virial coefficients B_2, B_3, and B_4 and their first two temperature derivatives were calculated as described below from the model intermolecular potentials ϕ and $\Delta\phi_3$. Next, Eq. (4), truncated after the fourth virial coefficient, was solved for the density corresponding to the temperature T_i and pressure p_i of the state point in question. Then $\{Z + \rho_n(\partial Z/\partial \rho_n)_T\}$, $\{Z + T(\partial Z/\partial T)_{\rho_n}\}$, and $C_{V,\text{m}}$ were calculated correct to the fourth virial coefficient from Eqs. (5a)–(5c), making use of the experimentally determined value of $C_{V,\text{m}}^{\text{pg}}(T_i)$, and finally, u was calculated from Eq. (2).

A slightly modified Levenberg–Marquardt algorithm was employed in the minimization of χ^2 [15]. This required values of the partial derivatives of $u_{\text{fit}}(T_i, p_i)$ with respect to each of the parameters which were determined numerically by first-order finite differences. However, since the computational effort required to evaluate B_4 and its temperature derivatives were large, while their contributions to u_{fit} were very small, these terms were held constant during a sequence of iterations. Once an apparent minimum in the χ^2 surface was reached, B_4 and its temperature derivatives were recalculated and the algorithm restarted. This procedure was repeated until satisfactory convergence was achieved.

The virial coefficients were calculated numerically by Gaussian quadrature. Expressions for the temperatures derivatives were obtained by differentiation of the integrands in Eqs. (11)–(13) and these quantities were then also calculated by quadrature. This approach avoids the need to calculate derivatives with respect to T by numerical differentiation and yields values of $T^i B_N^{(i)}$ with an accuracy similar to that of B_N itself.

In the case of B_2 and each of its temperature derivatives, the integral over r_{12} was divided into the following three regions: $[0, r_1]$, $[r_1, r_2]$, and $[r_2, \infty]$, where r_1 is the solution of $\phi(r_1)/kT = +30$ and $r_2 = 16 r_{\text{m}}$. In the first of these regions, e_{12} is negligibly small and the integral may be

evaluated analytically. In the last region, $\phi/kT \ll 1$ and $\phi \sim r^{-6}$ so that $f_{12} \approx \{-\phi(r_2)/kT\}(r_2/r)^6$ and the integral may also be evaluated analytically. The remaining region was divided into six equal panels and a 200-interval Gauss–Legendre quadrature formula was applied to each. This procedure was sufficient to yield a numerical accuracy of order $\pm 10^{-6}$ in $B_2^* = B_2/b_0$, where $b_0 = 2\pi L\sigma^3/3$ and σ is the value of r at which ϕ crosses zero.

Since the molecules are identical, the domain of integration for B_3 and its temperature derivatives may be restricted by holding $r_{12} \geqslant r_{13} \geqslant r_{23}$ so that [16]

$$V^{-1}\int_V dr_1\, dr_2\, dr_3 = 48\pi^2 \int_0^{\infty} r_{12}\, dr_{12} \int_{(1/2)r_{12}}^{r_{12}} r_{13}\, dr_{13} \int_{r_{12}-r_{13}}^{r_{13}} r_{23}\, dr_{23} \qquad (16)$$

The semiinfinite integral over r_{12} was truncated at $r_{12} = 8r_m$ and the remaining region was divided into two domains specified by r_{12} on $[0, r_1]$ and $[r_1, 8r_m]$, where r_1 is as defined above. In the first of these domains, all e_{ij}'s were set equal to zero and the integral was evaluated analytically. The integrals in the remaining domain were evaluated by Gauss–Legendre quadrature, with 200 intervals for r_{12} and 25 intervals each for r_{13} and r_{23}. This procedure was sufficient to achieve a numerical accuracy of order $\pm 10^{-4}$ in $B_3^* = B_3/b_0^2$. The small remaining numerical uncertainty appears to arise mainly from the nonadditive part of C, for which the integral converges rather slowly. However, this uncertainty has negligible effect in the present calculations.

To evaluate B_4 or one of its temperature derivatives, a sixfold integral must be enumerated, and to do this by direct quadrature requires the investment of a significant computational effort. Efficient algorithms for the evaluation of such integrals have been described [14, 17, 18]. However, as these require a partial expansion of the integrand in Legendre polynomials, which is slow to converge at the low reduced temperatures considered here, an approach based on direct quadrature was preferred. The semiinfinite radial integrals were each truncated at $r_{ij} = 5\sigma$, subdivided into a number of panels, and evaluated by Gaussian quadrature. The integrals over $\cos\theta_3$ and $\cos\theta_4$ were each enumerated in a single panel by Gauss–Legendre quadrature, while the integral over φ_4 was evaluated by Gauss–Chebchev quadrature taking advantage of the symmetry of the integrand about $\varphi_4 = \pi$. After careful tests, quadrature parameters were found that gave a satisfactory compromise between speed and accuracy. For the radial integrals, four panels were used with r/σ as follows: [0, 0.7] with 10 intervals, [0.7, 1.3] with 20 intervals, [1.3, 2.0] with 10 intervals, and [2.0, 5.0] with 20 intervals. In the case of each angular integral, 30 quadrature intervals were used. The estimated numerical uncertainty of $B_4^* = B_4/b_0^3$ is the

larger of 10^{-3} and 1%; this has a negligible effect in the present calculations. The method was also tested for the case of a pairwise additive Lennard–Jones system and the results were in good agreement with those of Henderson and Oden [18]. To minimize the computational effort, all terms contributing to B_4 and $T^i B_4^{(i)}$ (for $i = 1, 2$) were calculated together and each of the nearly 6×10^9 geometric configurations was therefore considered only once at each temperature.

4. THE FIT TO THE SPEED OF SOUND

Experimental speeds of sound in propane were available on seven isotherms at temperatures between 225 and 375 K with pressures up to the lesser of 0.85 MPa and 80% of the vapor pressure [11]. This corresponds to amount-of-substance densities no greater than about $0.37\ \text{mol} \cdot \text{dm}^{-3}$ and justifies the neglect of virial coefficients higher than the fourth. As a numerical example, the leading four terms in the series for Z as calculated from the final model at $T = 300$ K and $\rho_n = 0.37\ \text{mol} \cdot \text{dm}^{-3}$ are 1, −0.14222, +0.00233, and −0.00006. The convergence remains very good even at lower temperatures, where C and D diverge toward $-\infty$, because of the rapid decline in the saturated-vapor density. The experimental data have a high precision and each isotherm is smooth to within a few parts per million. Furthermore, the values of $C^{\text{pg}}_{T,\text{m}}(T_i)$ used in the analysis were those obtained by Trusler and Zarari [11] from an extrapolation of the same speeds of sound to the limit of zero density, where $u^2 = RT(C^{\text{pg}}_{T,\text{m}} + R)/MC^{\text{pg}}_{T,\text{m}}$. Since the use of these values forces agreement between the model and the data in the limit of zero density, the appropriate standard deviation for use in connection with Eq. (15) is one based on the estimated uncertainty of u/u_0 on each isotherm, where $u_0 = \text{Lim}_{p \to 0}(u)$. Accordingly, s_i was set equal to 0.002 m/s (approximately 10 ppm) for all points and this figure encompasses both the observed precision of the data and the uncertainty propagated from the estimated uncertainties in temperature and pressure.

It was found that the results were sensitive to the parameters ε, r_m, and ν_{123} and to one but not both of the parameters m and γ. Accordingly, γ was constrained somewhat arbitrarily to the value 10 and the remaining four parameters (ε, r_m, m, and ν_{123}) were optimized in the regression analysis. Crude initial values for the parameters in the pair potential came from a preliminary fit to the second acoustic virial coefficients of propane [19, 20]. The initial value of the three-molecule dispersion coefficient ν_{123} was estimated from the relation

$$\nu_{123} = 3\alpha C_6/4 \tag{17}$$

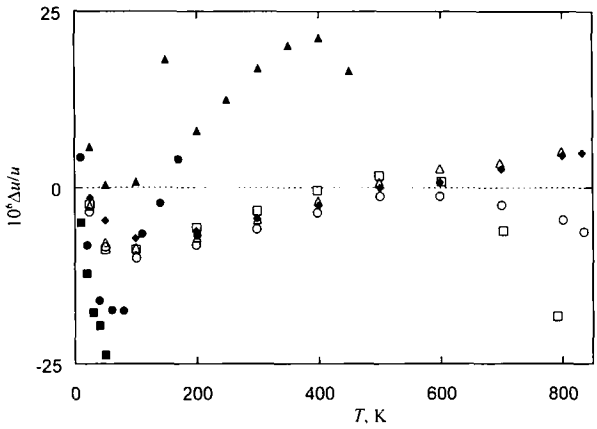

Fig. 2. Fractional deviations $\Delta u/u$ of experimental speeds of sound from the fit: ■, 225 K; ●, 250 K; ▲, 275 K; □, 300 K; ○, 325 K; △, 350 K; ◆, 375 K.

where α is the mean polarizability of the molecule and C_6 is the leading isotropic two-molecule dispersion coefficient. In the present case, α was estimated from the refractive index and C_6 was set equal to the coefficient of r^{-6} in Eq. (7) evaluated at $r = r_m$. The crude initial parameters were first refined during a regression analysis in which B_4 and its temperature derivatives were neglected entirely. This led to the following "initial" values:

$$\left.\begin{aligned} r_m &= 0.48430 \text{ nm} \\ \varepsilon/k &= 566.30 \text{ K} \\ m &= 69.5586 \\ \gamma &= 10 \\ \nu_{123}/k &= 0.04732 \text{ K} \cdot \text{nm}^9 \end{aligned}\right\} \tag{18}$$

Then B_4 and its temperature derivatives were calculated and the final analysis was started. This full analysis resulted in only small changes in the parameters and it was therefore necessary to recalculate the terms involving B_4 only once. The final values obtained for the parameters are as follows:

$$\left.\begin{aligned} r_m &= 0.48620 \text{ nm} \\ \varepsilon/k &= 560.56 \text{ K} \\ m &= 67.0328 \\ \gamma &= 10 \\ \nu_{123}/k &= 0.04589 \text{ K} \cdot \text{nm}^9 \end{aligned}\right\} \tag{19}$$

The standard deviations of the fit was $0.002\ \mathrm{m \cdot s^{-1}}$, the maximum absolute deviation was $0.006\ \mathrm{m \cdot s^{-1}}$, and $\chi^2 = 1.3$.

The deviations of the experimental speeds of sound from those given by the final model are shown in Fig. 2. It is clear that, while very small in absolute terms, there are some systematic deviations from the model which exceed the imprecision of the data. However, those deviations cannot be ascribed definitely to limitations in the model, as the value of χ^2 indicates that the data are fitted essentially within their overall uncertainty. Attempts to eliminate or reduce the deviations by adoption of an alternative potential model failed. For example, when fits were made with γ constrained to values other than 10, there was almost no change in the deviations, and although m changed, the overall potential model obtained was almost-identical to that reported here. The situation depicted in Fig. 2 is therefore considered to be the best that can be achieved by the methods employed here.

5. THE EQUATION OF STATE

The coefficients of the truncated virial equation of state proposed here for propane are specified, through the relations in Section 2, by the five parameters given in Eqs. (19). However, as this is not a particularly efficient route for repetitive calculations, the equation of state is presented here in the form of a look-up table for the virial coefficients and their first two temperature derivatives together with a specified method of interpolation.

To retain a high numerical accuracy without the use of an excessively large look-up table, a change of variables was made from T to the reduced reciprocal temperature $\tau = \varepsilon/kT$ in terms of which

$$\left.\begin{aligned} T\frac{dB_N}{dT} &= -\tau\frac{dB_N}{d\tau} \\ T^2\frac{d^2B_N}{dT^2} &= \tau^2\frac{d^2B_N}{d\tau^2} + 2\tau\frac{dB_N}{d\tau} \end{aligned}\right\} \tag{20}$$

This is especially advantageous for B_2, which is nearly linear in τ and is also the term required with the greatest accuracy. The results, in the dimensionless form of B_N^* and each of its first three derivatives with respect to τ, are given in Table I for the interval $0.8 \leqslant \tau \leqslant 2.8$ (corresponding approximately to the temperature range 200 to 700 K).

Table I. Reduced Virial Coefficients $B_N^* = B_N/b_0^{N-1}$ and Derivatives $\bar{B}_N^{*(l)} = (d^l B_N^*/d\tau^l)$; $b_0 = 0.12868\ \mathrm{dm^3 \cdot mol^{-1}}$, $\tau = (560.56\ \mathrm{K})/T$

τ	B_2^*	$\bar{B}_2^{*(1)}$	$\bar{B}_2^{*(2)}$	$\bar{B}_2^{*(3)}$	B_3^*	$\bar{B}_3^{*(1)}$	$\bar{B}_3^{*(2)}$	$\bar{B}_3^{*(3)}$	B_4^*	$\bar{B}_4^{*(1)}$	$\bar{B}_4^{*(2)}$	$\bar{B}_4^{*(3)}$
0.8	−0.28571	−1.86093	−0.96176	−0.56571	0.5044	0.5350	1.6266	−0.4323	0.043	−0.323	−0.426	59.8
0.9	−0.47671	−1.96010	−1.02316	−0.66015	0.5659	0.6942	1.5408	−1.3317	0.013	−0.244	1.502	12.7
1.0	−0.67795	−2.06586	−1.09352	−0.74627	0.6428	0.8399	1.3512	−2.5254	−0.003	−0.055	2.326	11.2
1.1	−0.89013	−2.17909	−1.17235	−0.83036	0.7331	0.9601	1.0231	−4.1171	0.005	0.226	3.260	9.3
1.2	−1.11404	−2.30061	−1.25965	−0.91603	0.8334	1.0386	0.5108	−6.2340	0.045	0.590	4.022	1.7
1.3	−1.35056	−2.43131	−1.35569	−1.00562	0.9387	1.0543	−0.2459	−9.0363	0.125	0.994	3.980	−10.9
1.4	−1.60064	−2.57206	−1.46096	−1.10082	1.0413	0.9790	−1.3255	−12.728	0.242	1.326	2.343	−39.6
1.5	−1.86534	−2.72383	−1.57609	−1.20297	1.1303	0.7755	−2.8291	−17.568	0.380	1.355	−2.576	−94.5
1.6	−2.14580	−2.88763	−1.70182	−1.31326	1.1906	0.3950	−4.8878	−23.890	0.489	0.645	−13.09	−102.0
1.7	−2.44330	−3.06457	−1.83905	−1.43283	1.2014	−0.2258	−7.6700	−32.119	0.459	−1.581	−33.65	−240.0
1.8	−2.75920	−3.25586	−1.98874	−1.56279	1.1348	−1.1698	−11.393	−42.801	0.078	−6.660	−71.49	−508.0
1.9	−3.09499	−3.46277	−2.15199	−1.70429	0.9532	−2.5444	−16.334	−56.631	−1.041	−16.83	−137.8	−875.0
2.0	−3.45232	−3.68675	−2.33002	−1.85856	0.6071	−4.4885	−22.852	−74.502	−3.576	−35.75	−250.2	−1,480.0
2.1	−3.83296	−3.92931	−2.52417	−2.02691	0.0308	−7.1819	−31.406	−97.557	−8.675	−69.35	−437.0	−2,440.0
2.2	−4.23886	−4.19217	−2.73592	−2.21073	−0.8617	−10.856	−42.584	−127.26	−18.25	−127.1	−742.5	−3,960.0
2.3	−4.67213	−4.47714	−2.96688	−2.41156	−2.1828	−15.810	−57.139	−165.47	−35.39	−224.0	−1234.0	−6,390.0
2.4	−5.13509	−4.78624	−3.21885	−2.63105	−4.0788	−22.428	−76.040	−214.61	−65.12	−383.6	−2018.0	−10,200.0
2.5	−5.63026	−5.12167	−3.49378	−2.87103	−6.7397	−31.203	−100.52	−277.72	−115.4	−642.5	−3252.0	−15,300.0
2.6	−6.16038	−5.48583	−3.79381	−3.13348	−10.412	−42.770	−132.18	−358.76	—	—	—	—
2.7	−6.72847	−5.88135	−4.12129	−3.42057	−15.413	−57.943	−173.04	−462.76	—	—	—	—
2.8	−7.33779	−6.31109	−4.47882	−3.73469	−22.154	−77.768	−225.71	−596.19	—	—	—	—

The recommended method of interpolation between adjacent points τ_1 and τ_2 is by means of the cubic polynomial $P(\tau)$ defined in that interval by

$$P(\tau) = a(\tau - \tau_1) + b(\tau - \tau_2) + \{c(\tau - \tau_1) + d(\tau - \tau_2)\}(\tau - \tau_1)(\tau - \tau_2) \quad (21)$$

The coefficients of this polynomial are chosen so as to reproduce exactly the tabulated values of the function f and its first derivative $f' = df/d\tau$ at both $\tau = \tau_1$ and $\tau = \tau_2$. Thus

$$\left.\begin{aligned} a &= f(\tau_2)/(\Delta\tau) \\ b &= -f(\tau_1)/(\Delta\tau) \\ c &= \{f'(\tau_2)/(\Delta\tau)^2\} - \{(a+b)/(\Delta\tau)^2\} \\ d &= \{f'(\tau_1)/(\Delta\tau)^2\} - \{(a+b)/(\Delta\tau)^2\} \end{aligned}\right\} \quad (22)$$

where f may be B_N or either its first or second derivative with respect to τ.

To permit interpolation of $d^2B_N^*/d\tau^2$, Table I includes values of the third derivatives $d^3B_N^*/d\tau^3$. For $N = 2$ or 3, $d^3B_N^*/d\tau^3$ was obtained from $d^3B_N^*/dT^3$ and the lower-order derivatives, while $d^3B_N^*/dT^3$ was evaluated by quadrature in the same way as described for B_N. However, $d^3B_4^*/d\tau^3$ was not calculated directly; instead, this quantity was determined by numerical differentiation of $d^2B_4^*/d\tau^2$.

The method of interpolation is highly accurate and ensures consistency between each term and the next higher derivative at all tabulated points. The accuracy of the method has been tested for $N = 2$ and 3 by comparing interpolated values with directly calculated results. In the cases of B_2, $TB_2^{(1)}$, and $T^2B_2^{(2)}$, the interpolation is accurate to within $10^{-6}\,\mathrm{dm^3 \cdot mol^{-1}}$ over the entire temperature range represented in Table I and this leads to negligible additional uncertainty in all thermodynamic properties at subcritical densities. For $N = 3$ and temperatures near 360 K, B_3 is given to within $\pm 0.4 \times 10^{-6}\,\mathrm{dm^6 \cdot mol^{-2}}$, $TB_3^{(1)}$ to within $\pm 4 \times 10^{-6}\,\mathrm{dm^6 \cdot mol^{-2}}$, and $T^2B_3^{(2)}$ to within $\pm 30 \times 10^{-6}\,\mathrm{dm^6 \cdot mol^{-2}}$. These figures correspond to numerical errors of 3 ppm in Z and 10 ppm in $C_{p,m}$ at the density of the saturated vapor (approximately $2.5\,\mathrm{mol \cdot dm^{-3}}$). At lower temperatures, the interpolation accuracy for B_3 and its derivatives deteriortates but the observable consequences of such errors remain negligible because of the rapid decline in the saturated vapor density. At higher temperatures, the interpolation accuracy improves. Interpolation errors in B_4 and its derivatives are thought to be insignificant compared with other uncertainties including the relatively low numerical accuracy to which these quantities were calculated in the first place.

All configurational thermodynamic properties of gaseous propane may be calculated from the equation of state model presented in this paper. The entries in Table I permit calculations to be made in the temperature range 200 to 700 K and it is argued below that the equation is useful at densities up to about $\rho_n^c/4$ over this entire temperature range ($\rho_n^c = 4.955$ mol · dm^{-3}) [22].

To obtain caloric properties, the heat capacity of the perfect gas (or equivalent information) is required. As discussed above, experimental results are available from the speed of sound data of Trusler and Zarari in the temperature range 225 to 375 K [11]. Wide-ranging results calculated from spectroscopic data are also available [21] but unfortunately they are about 0.4% greater than the experimental data in the overlapping temperature range. The differences considerably exceed the experimental uncertainties (which include an allowance for the possible presence of undetected impurities) and therefore suggest that some revision of the calculated values may be needed. For the present, the correlation given by Trusler and Zarari is recommended [11]:

$$C_{p,\mathrm{m}}^{\mathrm{pg}}/R = -0.4362 + 8.1447\theta + 1.1532\theta^{-1} \tag{23}$$

Here $\theta = T/(300\ \mathrm{K})$ and the correlation is valid in the temperature range 225 to 375 K.

6. COMPARISON WITH OTHER EXPERIMENTAL DATA

The truncated virial equation of state together with the experimental perfect-gas heat capacities provide a very precise representation of the experimental speeds of sound. Even when Eq. (23) is used in place of the experimental value of $C_{p,\mathrm{m}}^{\mathrm{pg}}$ on each isotherm, the agreement is always within 0.01%. In the region of temperature and density in which the model has been optimized, it is likely that all the thermodynamic properties are given with a very high accuracy but there are really very few other experimental data in that region against which to test this assertion. However, the equation of state can be severely tested by comparison with the pVT data of Thomas and Harrison [22], which, for the gas phase, refer to the region $323.15 \leqslant T \leqslant 623.15$ K and $\rho_n \geqslant 0.8$ mol · dm^{-3}. A comparison with those results involves an extrapolation to at least twice the greatest density used in the fitting procedure and may be used both to test the ability of the model to extrapolate upward in temperature and density and, by inference, to estimate the uncertainty at lower densities.

Figure 3 shows deviations ΔZ of the experimental compression factors reported by Thomas and Harrison from those calculated from the present

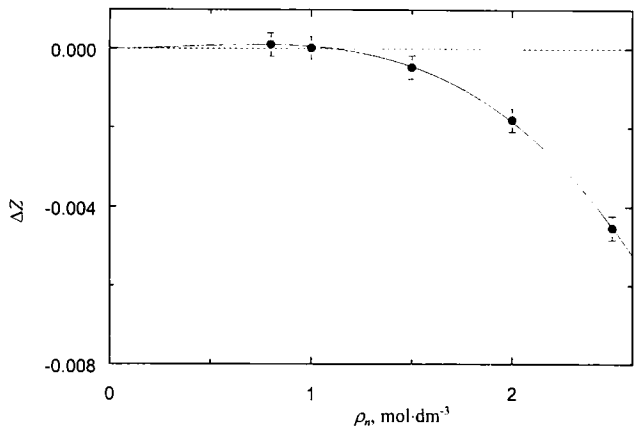

Fig. 3. Deviations ΔZ of experimental compressions factors [22] from the predictions of the model on the critical isotherm. ●, ΔZ; ——, fit to $\Delta Z = c\rho_n^2 + d\rho_n^3$.

equation of state on the critical isotherm ($T^c = 369.85$ K) at densities up to 2.5 mol · dm^{-3}. In the upper half of this range, there are deviations which substancially exceed the experimental uncertainty of $\pm 3 \times 10^{-4} Z$. An interpolation indicates that ΔZ exceeds this uncertainty when $\rho_n >$ 1.35 mol · dm^{-3} or, conversely, that for $\rho_n \leqslant 1.35$ mol · dm^{-3} the equation of state agrees with the experimental data. The disagreement reaches 0.1 % at $\rho_n \approx 1.6$ mol · dm^{-3}. Figure 4 shows ΔZ as a function of T for the four

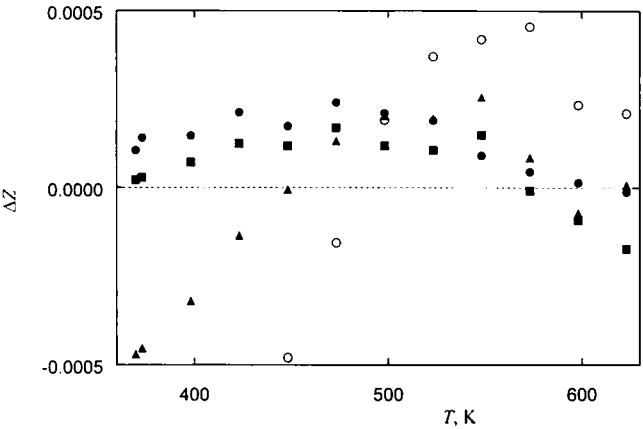

Fig. 4. Deviations ΔZ of experimental compression factors [22] from the predictions of the model on four isochores: ●, 0.8 mol · dm^{-3}; ■, 1.0 mol · dm^{-3}; ▲, 1.5 mol · dm^{-3}; ○, 2.0 mol · dm^{-3}.

lower isochores reported by Thomas and Harrison: $\rho_n/(\text{mol}\cdot\text{dm}^{-3}) = 0.8$, 1.0, 1.5, and 2.0. The evidence of this figure suggests that the present equation of state is not in error by more than 0.03% in the whole region above the critical temperature at densities up to at least $\rho_n^c/4$.

In the subcritical region, there are very few data with which to compare the equation of state. Thomas and Harrison report vapor pressures p^σ for $T \geqslant 258.15$ K and saturated vapor densities ρ_n^σ for $T \geqslant 323.15$ K. The present equation of state applies only to the gas phase and cannot therefore be solved for vapor–liquid equilibrium. However, the density corresponding to the experimentally determined p^σ may be calculated and a comparision of the results with the experimental ρ_n^σ indicates agreement to within 0.04% at $T = 323.15$ K (where $\rho_n^\sigma \approx \rho_n^c/5.6$) and to within 0.1% at 333.15 K (where $\rho_n^\sigma \approx \rho_n^c/4.4$). At higher temperatures, and thus high densities, the calculated values diverge from the experimental results. This comparison therefore indicates that the equation of state comes into agreement with the experimental results at subcritical temperatures when ρ_n falls below about $\rho_n^c/5$. A reasonable conclusion to draw from this comparison is that the equation of state is correct to within about 0.04% in Z at temperatures near 323.15 K for all densities up to ρ_n^σ; indeed, the accuracy is most probably very much better at lower densities.

Although errors in the virial coefficients may grow rapidly as the model is extrapolated to low temperatures, the decline in the saturated vapor density appears to be such that the consequences of such errors for predictions of vapor-phase properties diminish. This is associated with the fact that the saturated vapor becomes more nearly ideal as the temperature

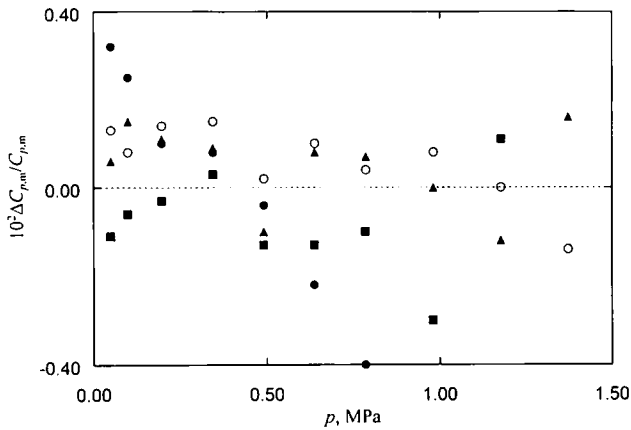

Fig. 5. Deviations $\Delta C_{p,m}$ of experimental isobaric heat capacities [23] from the predictions of the model: ●, 293.15 K; ■, 313.15 K; ▲, 333.15 K; ○, 353.15 K.

is lowered despite the divergence of the virial coefficients. Thus the model is expected to be reliable at temperatures at least down to 200 K.

Apart from virial coefficients, which are discussed briefly below, the only other precise experimental data available in the subcritical region are the isobaric heat capacities reported by Ernst and Büsser [23], which have a claimed uncertainty of 0.1%. These data are compared in Fig. 5 with the predictions based on the present equation of state with $C_{p,\mathrm{m}}^{\mathrm{pg}}$ from Eq. (23); the agreement is generally within 0.2%. The results on the isotherm at 293.15 K agree rather less well and deviate by about 0.4% in the limit of zero pressure. That deviation far exceeds the uncertainty of Eq. (23) and suggests that there may be errors in the caliometric data that significantly exceed the uncertainty.

7. THE VIRIAL COEFFICIENTS OF PROPANE

As a result of this study and the earlier work of Thomas and Harrison [22] both the second and the third virial coefficients of propane appear to be well established at temperatures between 225 and 623.15 K. As shown in Fig. 6, the model pair potential predicts second virial coefficients that agree very closely with those of Thomas and Harrison over the entire temperature range studied by the latter. Comparisons with other values of B_4 available in the literature were also generally good [24]. The estimated uncertainty of the calculated second virial coefficients is 0.002 $\mathrm{dm^3 \cdot mol^{-1}}$ at 225 K, declining to 0.0005 $\mathrm{dm^3 \cdot mol^{-1}}$ at 300 K and to 0.0002 $\mathrm{dm^3 \cdot mol^{-1}}$ for $T \geqslant 350$ K. These uncertainty estimates are based on the following three considerations: first, the changes in B_2 found when an alternative model

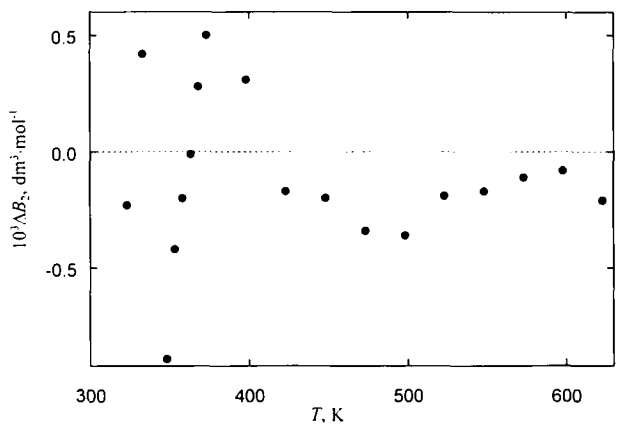

Fig. 6. Deviations ΔB_2 of experimental second virial coefficients [22] from the predictions of the model.

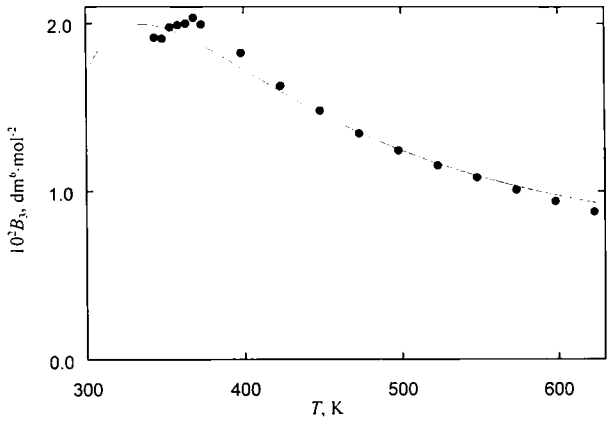

Fig. 7. Comparison of experimental and predicted third virial coefficients: ——, predicted; ●, experimental [22].

pair potential was fit to the speed of sound; second, the changes when terms in the fourth virial coefficient were dropped from the fit; and third, a comparison with the results of Thomas and Harrison.

The predicted values of B_3 are compared with those of Thomas and Harrison in Fig. 7 and the agreement must be regarded as good. The estimated uncertainty in the predicted third virial coefficients, obtained in the same way as for B_2, varies from 0.001 dm$^6 \cdot$ mol^{-2} at 225 K to 0.0003 dm$^6 \cdot$ mol^{-2} at 623.15 K.

Figure 8 shows the present values of B_4 in comparison with those reported by Thomas and Harrison. Clearly, there is little agreement in this

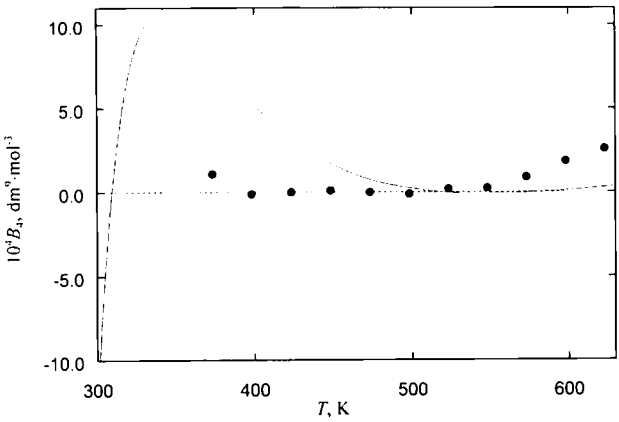

Fig. 8. Comparison of experimental and predicted fourth virial coefficients: ——, predicted; ●, experimental [22].

case. Since the experimental fourth virial coefficients reported in Ref. 22 appear to be consistent with the pVT data and significant in the light of the claimed uncertainties, the tentative conclusion is that the present model fails at the fourth virial coefficient.

Interestingly, values of B_2 and B_3 predicted by the model with parameters from Eqs. (18), obtained under the assumption $B_4 = 0$, are in equally good agreement with experiment.

8. PROPERTIES OF THE SATURATED VAPOR

No accurate measurements of the properties of saturated propane vapor, other than of the vapor pressure itself, are available for temperatures below 323.15 K. Consequently, it would seem useful to calculate saturation properties from the combination of the present model with an expression for the saturated vapor pressure. Such calculations have been made for the temperature range 258.15 to 323.15 K with vapor pressures from the smoothing equation given in Ref. 22 and the results are presented in Table II. Based on the comparisons given above and the uncertainty of the vapor pressure equation [22], the density and compression factor of the saturated vapor should not be in error by more than about 0.05%. A similar uncertainty should be attached to the speed of sound. The uncertainty of the isochoric heat capacity is more difficult to estimated but is probably not more than 0.2%.

Table II. Properties of Saturated Propane Vapor

T (K)	p (MPa)	ρ_n (mol·m^{-3})	Z	$C_{p,m}/R$	$C_{V,m}/R$	u (m·s^{-1})
258.15	0.29189	147.58	0.92144	7.1919	8.6290	221.814
260.00	0.31092	156.69	0.91792	7.2433	8.7041	221.847
265.00	0.36709	183.51	0.90788	7.3842	8.9150	221.794
270.00	0.43057	213.80	0.89710	7.5280	9.1385	221.524
275.00	0.50194	247.89	0.88556	7.6749	9.3763	221.029
280.00	0.58177	286.18	0.87322	7.8249	9.6305	220.297
285.00	0.67065	329.07	0.86007	7.9781	9.9035	219.319
290.00	0.76919	377.04	0.84607	8.1348	10.1984	218.082
295.00	0.87798	430.66	0.83119	8.2950	10.5194	216.573
300.00	0.99768	490.54	0.81538	8.4590	10.8715	214.780
305.00	1.12891	557.44	0.79859	8.6272	11.2618	212.686
310.00	1.27234	632.24	0.78077	8.8000	11.6993	210.274
315.00	1.42866	716.03	0.76182	8.9776	12.1962	207.526
320.00	1.59860	810.13	0.74165	9.1606	12.7702	204.421
323.15	1.71299	875.44	0.72826	9.2794	13.1825	202.272

9. CONCLUSIONS

The results presented in this paper comprise an accurate equation of state for gaseous propane at densities up to about one-quarter of the critical. Below about 1 mol · dm^{-3}, the results are believed to be more accurate than previous correlations, but above about 1.5 mol · dm^{-3} the predictions of the model start to deviate significantly from experimental data.

Based on these results, it appears that a simple isotropic model of the pair potential, coupled with the Axilrod–Teller triple-dipole term, can provide an accurate description of the equation of state up to the third virial coefficient. There is evidence that the model fails at the fourth virial coefficient. Since the discrepancies shown in Fig. 8 are large compared with the calculated nonadditive contribution to B_4, the failing might be due to the approximate treatment of pairwise intermolecular forces. That failing might be attributed in turn to either or both of the main assumptions: that the molecular framework is rigid and that the potential is isotropic. Resolution of that issue would require calculations of B_4 for more realistic potential models. In the meantime, it appears that inclusion of fourth virial coefficients in a procedure such as that described here offers little advantage. The alternative approach of abandoning a single pair potential in favor of the use of different models to represent some virial coefficients has been considered [10]. While evidently more empirical, this would probably permit an improved representation of B_4. However, in the present case, the acoustic data upon which the fit was based do not extend to sufficiently high densities to justify the inclusion of additional parameters pertaining only to virial coefficients beyond the third.

Although beyond the scope of this work, it is also clear that the addition to the truncated virial series of a small number of empirical terms would permit greatly improved representation of the pVT surface at higher densities.

REFERENCES

1. M. R. Moldover, J. B. Mehl, and M. Greenspan, *J. Acoust. Soc. Am.* **79**:253 (1986).
2. J. P. M. Trusler and M. Zarari, *J. Chem. Thermodyn.* **24**:973 (1992).
3. A. F. Estrada-Alexanders, J. P. M. Trusler, and M. P. Zarari, *Int. J. Thermophys.* **16**:663 (1995).
4. A. F. Estrada-Alexanders, Ph.D. thesis (University of London, London, 1996).
5. A. F. Estrada-Alexanders and J. P. M. Trusler, *Int. J. Thermophys.* **17**:1325 (1996).
6. J. P. M. Trusler, Unpublished calculations.
7. B. E. Gammon, *J. Chem. Phys.* **64**:2556 (1976).
8. M. B. Ewing, A. R. H. Goodwin, M. L. McGlashan, and J. P. M. Trusler, *J. Chem. Thermodyn.* **20**:243 (1988).
9. J. P. M. Trusler, *J. Chem. Thermodyn.* **26**:751 (1994).

10. K. A. Gillis and M. R. Moldover, *Int. J. Thermophys.* **17**:1305 (1996).
11. J. P. M. Trusler and M. P. Zarari, *J. Chem. Thermodyn.* **28**:329 (1996).
12. E. A. Mason and T. H. Spurling, *The Virial Equation of State* (Pergamon Press, Oxford, 1969).
13. G. C. Maitland and E. B. Smith, *Chem. Phys. Lett.* **22**:443 (1973).
14. R. J. Dulla, J. S. Rowlinson, and W. R. Smith, *Mol. Phys.* **21**:229 (1971).
15. P. R. Brevington, *Data Reduction and Error Analysis for the Physical Sciences* (McGraw-Hill, New York, 1969), pp. 232–246.
16. A. E. Sherwood and J. M. Prausnitz, *J. Chem. Phys.* **41**:413 (1964).
17. J. A. Barker and J. J. Monaghan, *J. Chem. Phys.* **36**:2564 (1962).
18. D. Henderson and L. Oden, *Mol. Phys.* **10**:405 (1966).
19. M. P. Zarari, Ph.D. thesis (University of London, London, 1993).
20. J. P. M. Trusler, W. A. Wakeham, and M. P. Zarari, *Int. J. Thermophys.* **17**:35 (1996).
21. J. Chao, R. C. Wilhoit, and B. J. Zwolinski, *J. Phys. Chem. Ref. Data* **2**:427 (1973).
22. R. H. P. Thomas and R. H. Harrison, *J. Chem. Eng. Data* **27**:1 (1982).
23. G. Ernst and J. Busser, *J. Chem. Thermodyn.* **2**:787 (1970).
24. J. H. Dymond and E. B. Smith, *The Virial Coefficients of Pure Gases and Mixtures* (Clarendon Press, Oxford, 1980).